Charged Particle Bombardment of Zirconium Alloys

A Review

Author

Ron Adamson
Fremont, CA, USA

A.N.T. INTERNATIONAL®

Advanced Nuclear Technology International
Analysvägen 5, SE-435 33 Mölnlycke
Sweden

info@antinternational.com
www.antinternational.com

Ecolabelled printed matter, 441 799

Disclaimer

The information presented in this report has been compiled and analysed by Advanced Nuclear Technology International Europe AB (ANT International®) and its subcontractors. ANT International has exercised due diligence in this work, but does not warrant the accuracy or completeness of the information. ANT International does not assume any responsibility for any consequences as a result of the use of the information for any party, except a warranty for reasonable technical skill, which is limited to the amount paid for this assignment by each Project programme member.

Acknowledgement

A sanity check, general review and technical comments were graciously provided by Dr Ted Darby of Rolls-Royce, U.K. His expert contributions are much appreciated and enthusiastically acknowledged. Any errors or omissions in the report, however, are solely the responsibility of the author.

Contents

1 Charged particle bombardment of zirconium alloys (Ron Adamson)

1.1 Overall introduction

The ability of reactor engineers to predict changes in the dimensions of the reactor core components during service is crucial to the safety and efficiency of reactor operation. Successful core design anticipates dimensional changes due to thermal expansion, stress-induced elastic deformation and, to some extent, large stress plastic deformation of core components. Of greater difficulty is predicting dimensional changes due to the effects of the intense irradiation environment, mainly due to high energy neutrons produced by the fission process. Fuel rods, spacers/grids, channels, guide tubes, tie rods, other structural components, etc. – all undergo irradiation-induced dimensional changes due to irradiation growth, irradiation creep, irradiation-altered plastic deformation, and irradiation-influenced corrosion and hydriding of the zirconium alloy components. These topics and processes are routinely covered by the ZIRAT programs, with specific reports listed Section 1.2.

The dimensional changes are all connected to irradiation.-induced changes in microstructure and microchemistry caused by irradiation. The creation point defects (vacancies (V_s), interstitials (SIA)), clusters of point defects, dislocation loops, and transmutations all contribute to the altered properties – all of which are covered in detail in previous ZIRAT reports. Examples include irradiation growth, which is independent of stress; irradiation creep, which is stress and neutron flux dependent; corrosion-induced hydriding, which depends on the difference in density of hydrides and zirconium.

Nearly all such data reported previously by ZIRAT concerns the effects of neutron irradiation. This current ZIRAT19 STR reviews the effect of charged particle bombardment[1] (or ion irradiation or ion bombardment, all used interchangeably in this report) on not only the standard dimensional stability topics but also the full range of properties that can be influenced by ion irradiation.

The primary questions addressed are:

1) What properties of zirconium alloys can ion irradiation simulate (emulate or substitute for) neutron irradiation?

2) How, or to what extent, can ion bombardment complement neutron irradiation?

1.2 Ion bombardment introduction

Many ZIRAT reports have dealt with the effects of reactor/neutron irradiation on the behaviour and properties of zirconium alloy reactor components. Included are:

- ZIRAT6 STR “Mechanical Properties of Zr Alloys”
- ZIRAT7 STR “Corrosion of Zr Alloys”
- ZIRAT7 STR “Dimensional Stability of Zr Alloys”
- ZIRAT10 STR “Structural Behaviour of Fuel and Fuel Channel Components”

[1] In this report charged particles, electrons and protons are called “ions”, although it is not strictly correct.

- ZIRAT10 STR "Effect of Irradiation on Material Performance"
- ZIRAT12 STR "Corrosion Mechanism of Zr Alloys"
- ZIRAT14 STR "In Reactor Creep of Zr Alloys"
- ZIRAT16 STR "Channel Distortion"
- ZIRAT15 AR, Section 4 "Mechanical Properties"
- ZIRAT17 AR, Section 5 "Irradiation Growth"

The extensive record of material performance as affected by neutron irradiation recognizes the large effort required to gather the requisite properties:

- 2-7 years in-reactor exposure
- several years for in-pool measurements or shipment to hot cells
- extensive effort and precautions needed to handle highly radioactive material
- several years for in-cell or in-laboratory examinations
- overall high cost of gathering data
- limited flexibility in sorting single experimental variables

During the current century, accelerated efforts have been made to "simulating" the effects of neutron irradiation by conducting ion "bombardment" (or "irradiation", used interchangeably in this report) to gather data. A list of most of such (or related) experiments on zirconium alloys since 1966 is given in Table 1-1. The list is given in chronological order.

Table 1-1: Chronological listing of relevant references.

Year	References
1960s	
1966	[Gulden & Berstein, 1966], [Adamson, 1966]
1970s	
1970	[Nelson et al, 1970]
1972	[Riley & Grundy, 1972]
1974	[Adamson et al, 1974], [Lee & Koch, 1974]
1978	[Mansur, 1978]
1980s	
1980	[Coleman et al, 1980]
1981	[Parson et al, 1981]
1983	[Parson et al, 1983]
1984	[Chapman et al, 1984]
1987	[Yang et el, 1987]
1988	[Hellio et al, 1988], [Parson & Hoelke, 1988], [Schuster & Lemaignan, 1988]
1989	[Lefebvre & Lemaignan, 1989], [Motta et al, 1989]
1990s	
1990	[Kai et al, 1990], [Lefebvre & Lemaignan, 1990]
1991	[Motta et al, 1991], [Phythian et al, 1991]
1992	[Kai et al, 1992]
1993	[Cann et al, 1993], [Griffiths et al, 1993]
1994	[Griffiths et al, 1994], [Pêcheur et al, 1994]
1995	[Zou et al, 1995], [Woo et al, 1995]
1996	[de Carlan et al, 1996], [Howe et al, 1996], [Motta et al, 1996]
1997	[Zou et al, 1997]
2000s	
2000	[Woo et al, 2000]
2004	[Chow et al, 2004]
2005	[Zu et al, 2005], [Hayashi et al, 2005]
2007	[Was, 2007]
2008	[Sarkar et al, 2008]
2009	[Fournier et al, 2009]
2011	[Tournadre et al, 2011], [Ziegler, 2011]
2012	[Hengstler-Eger et al, 2012], [Onimus & Béchade, 2012], [Une et al, 2012], [Yamada & Kameyama, 2012]
2013	[Campbell & Was, 2013], [Gharbi et al, 2013], [Idrees et al, 2013a], [Idrees et al, 2013b], [Janse van Vuuren et al, 2013], [Oono et al, 2013], [Tournadre et al, 2013a], [Tournadre et al, 2013b], [Xu et al, 2013], [Zhang et al, 2013]
2014	[Hengstler-Eger et al, 2014], [Sonada et al, 2014]
	ANT International, 2014

Advantages in using ion irradiations include:

- high damage rates, allowing irradiation doses relevant to in-reactor performance to be reached in hours or days
- relatively low overall cost
- radiation activation absent or relatively low
- potential to control experimental variables (temperature, dose or fluence, compositions)
- in-situ (e.g. real time TEM observations) experiments possible
- short experimental "turn-around time" may allow iteration based on "what is learned"

Disadvantages in using ion irradiations include:

- high damage rates
  - is property being studied sensitive to damage rate?
  - how is the effective temperature (temperature shift, see Section 1.2.3) affected
- short ion penetration lengths introduce surface effect issues (surfaces attract both ions and point defects)
- ion beams are often rastered to produce uniform damage on a specimen
  - average and instantaneous damage rates can be different

Table 1-2 summarises advantages and disadvantages of various ions used for bombardments.

Table 1-2: Comparison of various particle-type irradiations, after [Was, 2007].

	Advantages	Disadvantages
Electrons	• TEM from standard HVEM • In-situ with TEM specimens • High dose rate and short irradiation time • High range-depth of penetration	• HVEM limited to 1 MeV • Van de Graff generators rare • Produces Frenkel pairs only – no cascades • Very high local heating • Large gradients in dose • Large temperature shift
Heavy Ions	• High dose rates – short irradiation times • Cascades similar to neutrons	• Very short penetration • Strongly peaked damage profile • Large temperature shift • Possible surface effects • Possible ion accumulation
Protons	• Moderate but accelerated dose rate • Moderate temperature shift • Relatively high penetration • Relatively flat damage profile over workable length	• Some small radio-activation • Small widely separated cascade • Possible hydride formation
		ANT International, 2014

1.2.1 Basic damage

In simplistic terms (described in excellent detail in the relatively recent book by [Was, 2007]) the initial radiation damage caused by a neutron, heavy ion or proton is the Brinkman displacement spike consisting of a vacancy (V) rich core surrounded by a shell of interstitials (SIAs). Slightly more realistic is the Seegar depleted (vacancy rich) zone. Both are shown in Figure 1-1. In the temperature ranges relevant to LWR materials, the results are clusters of V_s or SIAs, individual V_s and SIAs (collectively called Frenkel pairs) and after some short time ($<10^{-10}$ seconds) vacancy and interstitial dislocation loops. Taken together, these are called "irradiation damage".

In the case of electron irradiations the electron mass is so low that little damage is created (as in the average case in-reactor) unless the electron energy is very high (1 MeV). Even in that case only Frenkel pairs are created.

No single type of radiation can exactly simulate neutron irradiation, as each has its own basic damage-creation characteristics. This is illustrated in Figure 1-2, adapted from [Was, 2007] for Ni. Electrons from a HVEM create only Frenkel pairs. The average energy transferred to a Zr atom in a "collision" $\overline{T}$, is 60 eV, which is only slightly more than the energy needed to displace the atom ($E_d \approx 40$ eV). This displacement efficiency ($\in$ = the fraction of Frenkel pairs which survive the collapse of the displacement spike or cascade) is near 100%, since no spikes are created. With electrons, very high beam currents are possible, allowing high damage rates and causing high local temperatures. 1 MeV protons do cause small, widely spaced cascades, and 25% of the Frenkel pairs survive. 1 MeV heavy ions create dense, large cascades, more similar to neutrons than the others. Although the goal of many current experiments is to "simulate" reactor neutron irradiation with ions and electrons, it is really a "different irradiation altogether" [Motta et al, 1996]. Relating to the effects of reactor irradiation is the challenge for the experimenter.

Another difference between reactor neutrons and accelerated ions is the respective energy spreads. For neutrons the energy range is from very low (0.03 eV for thermal neutrons) to several MeV. For ions, the beam is almost mono-energetic with a very narrow energy spread. For electrons there is a Gaussian energy distribution with a wide enough spread that could result in dose gradients across the beam.

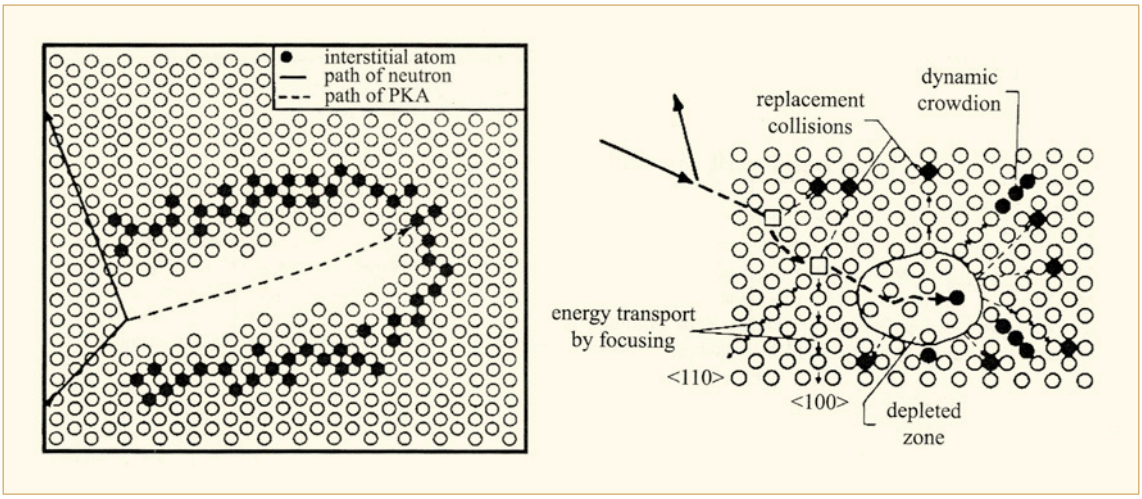

Figure 1-1: Displacement spike (cascade) [Brinkman, 1956] and revised by [Seegar, 1958].

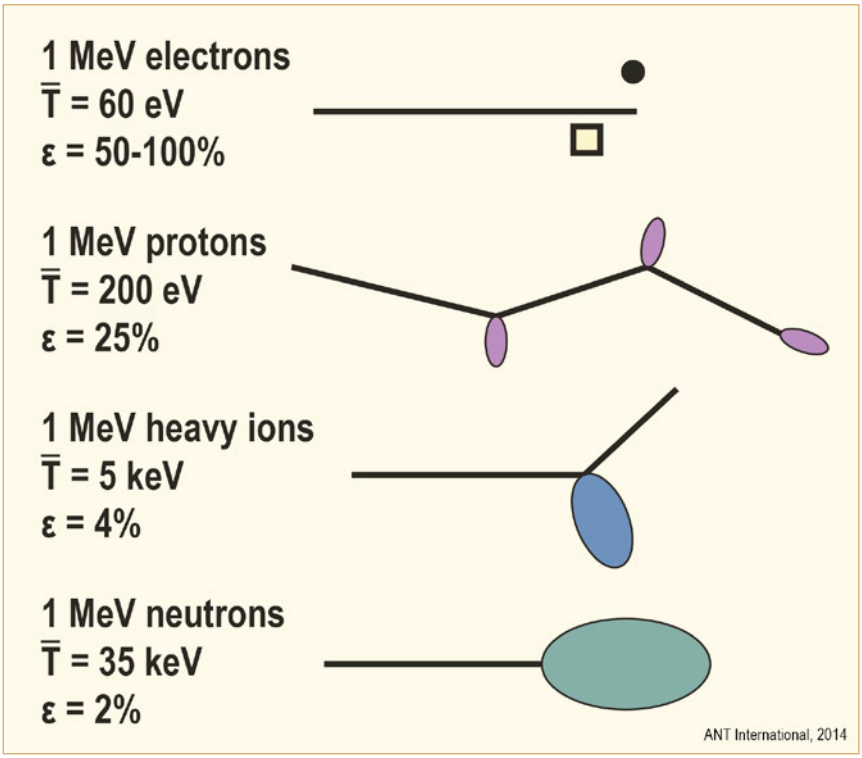

Figure 1-2: Difference in damage morphology, displacement efficiency (∈), and average recoil energy ($\bar{T}$) for 1 MeV particles incident on Ni, after [Was & Allen, 1994].

1.3 Initial studies

[Gulden & Berstein, 1966] were probably the first to apply ion bombardment to produce irradiation damage in zirconium. Irradiation (bombardment[3]) with krypton (Kr) produced no damage visible initially in the TEM, but after post-irradiation annealing some dislocation loops (actually black spots) were observed. Shortly thereafter, ion bombardment techniques were successfully used to study irradiation damage in several different fast reactor materials, particularly initiation and growth of irradiation-induced voids [Corbett & Ianniello, 1972] and [Nelson et al, 1970]. And, a small study [Riley & Grundy, 1972] indicated that low energy Kr ions produced irradiation damage that appeared to be similar to that produced by neutron irradiation at 400°C (673 K).

The first extensive ion bombardment studies on zirconium alloys were conducted by General Electric metallurgists in the early 1970s [Lee & Koch, 1974] and [Adamson et al, 1974].

Irradiation parameters were:

- 45.5 MeV Ni^{+6}, dose rate 2.5×10^{-4} dpa/s
- 5.0 MeV Ni^{+2}, dose rate 1.7×10^{-2} dpa/s
- BWR neutrons, dose rate 7.0×10^{-8} dpa/s

Dose rates were calculated using techniques developed at the time (see [Lee & Koch, 1974] for details). They are internally consistent, but differ somewhat from calculations done today.

The calculated typical damage-depth curves are given in Figure 1-22 and Figure 1-23. (More details on penetration are given in Section 1.5.2) It is noted that the dpa versus penetration is very steep for 5 MeV Ni and less so for 46 MeV Ni. In both cases however the exact location of examination in the TEM foil is crucial for quantitative assessment of local dpa. Also it is likely that Ni lodges in the foil since the average range is near the peak in the dpa curve (Figure 1-23).

[3] In this report, "irradiation" and "bombardment" is used interchangeably.

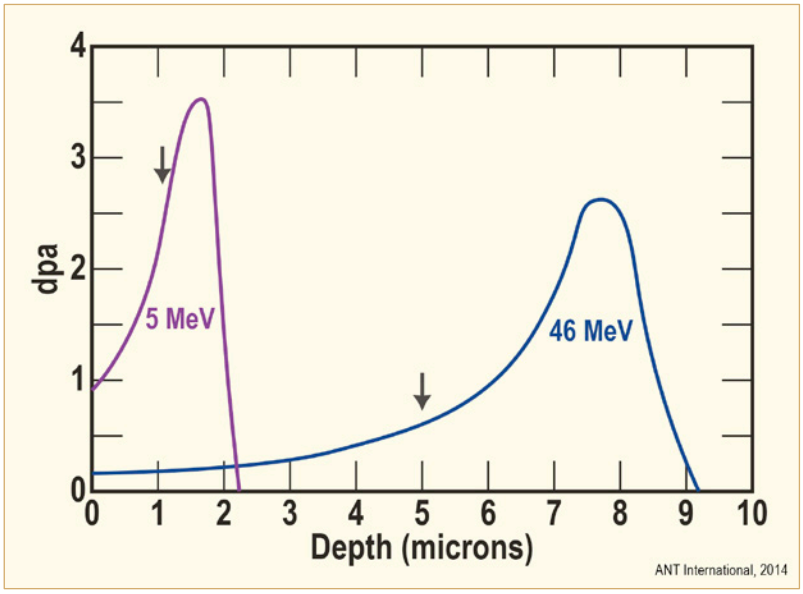

Figure 1-22: dpa versus depth for 1×10^{15} nickel ions/cm^2 incident upon zirconium. Arrows mark the location of TEM examinations, after [Adamson et al, 1974].

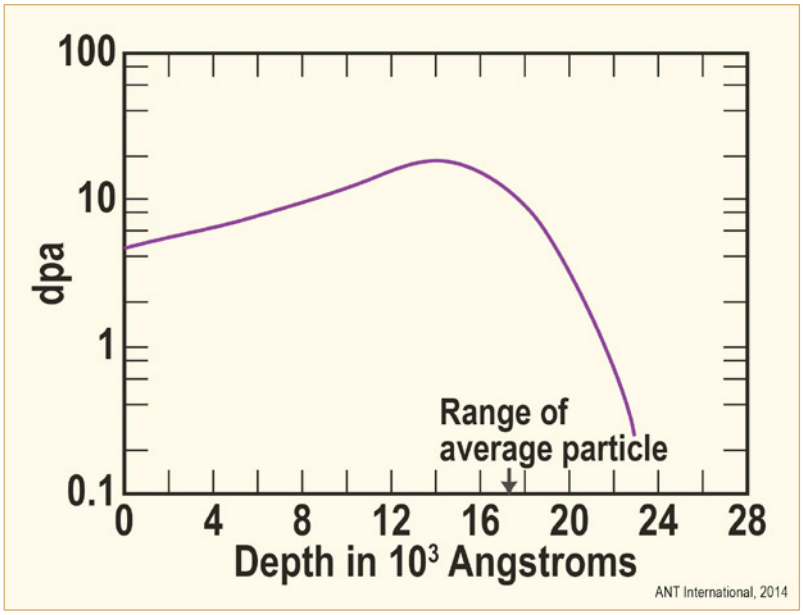

Figure 1-23: dpa versus depth for 1×10^{16} Ni ions/cm^2 having energy of 5 MeV incident on Zr. Range of the average Ni ion is also shown, after [Lee & Koch, 1974].

In the 5 MeV Ni bombarded specimens, many strange features were observed, including clear alignment of "defects" on the basal plane. It is very likely that implanted Ni was related to these structures.

For bombardment temperature between 500-600°C (773-873 K) severe annealing of the radiation damage occurs. As discussed in Section 1.2.3. Temperature shift, this indicated that temperature shifts calculated to be 150-250°C (150-250 K) are too large.

The GE authors suggest that for Ni ion irradiation, 400°C is about the right temperature to simulate typical BWR or PWR reactor irradiations. This agrees with the very early conclusion of [Riley & Grundy, 1972] for bombardment with Kr ions.

1.4 Amorphization of SPPs

At normal light water reactor temperatures (270-370°C (543-643K)) the SPPs change under neutron irradiation in a combination of two ways – amorphization and dissolution. For the Laves phase SPP, the amorphization process begins at the outside surface of the SPP, is connected with a significant decrease of the Fe/Cr ratio, and works its way inward with increasing fluence. The Zr_2(Fe,Ni) (sometimes incorrectly called Zintle) phase SPP does not become amorphous but does dissolve, as detailed below. At typical LWR operating temperatures, both SPPs dissolve relentlessly until the SPP essentially disappears. As SPPs dissolve, the zirconium matrix becomes enriched (well beyond the normal solubility limit) in the dissolving element.

Amorphization means that the original SPP crystalline structure is converted to an amorphous structure. Amorphization is a complex process, described in some detail by [Griffiths et al, 1987], [Yang, 1989], [Motta et al, 1996], [Motta, 1997], [Bajaj et al, 2002], [Taylor et al, 1999] etc. It occurs when an intermetallic compound accumulates enough irradiation-induced defects to cause it to thermodynamically favour an amorphous rather than a crystalline structure. The rate of amorphization depends on the relative rates of damage creation and damage annealing in the SPP; therefore important parameters are damage rate (neutron flux), irradiation temperature and SPP chemistry. A critical temperature exists above which the annealing processes are fast enough to prevent the accumulation of defects needed for transformation. For reactor irradiations amorphization of both $Zr(FeCr)_2$ and Zr_2(FeNi) occurs readily at temperatures near 100°C (373K) (although, and partly because, Fe is not released from the SPPs into the Zr matrix, to be discussed below). At typical light water reactor (LWR) temperatures (about 300°C (573K)) and neutron fluxes, $Zr(Fe,Cr)_2$ becomes amorphous but Zr_2(FeNi) does not. Above about 330°C (603K), neither SPP becomes amorphous.

As introduced above, the amorphization process begins at the outside surface of the SPP and works its way inward with increasing fluence. This is illustrated in Figure 1-25 [Etoh & Shimada, 1993], where the SPP on the left has an amorphous rim (dark area) and the one on the right, at higher fluence, is fully amorphous. There appears to be an incubation period prior to initiation of amorphization, with the incubation fluence decreasing with decreasing temperature in the range 270-330°C (543-603K).

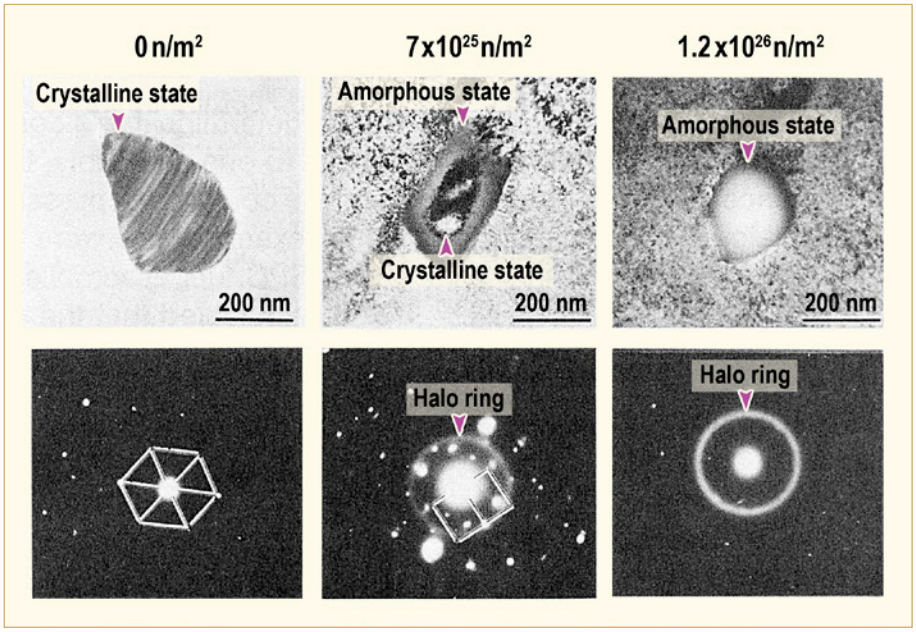

Figure 1-25: The fluence dependence of the amorphous transformation of $Zr(Fe,Cr)_2$ precipitate in RXA Zircaloy-2, neutron irradiated at 288°C(561K). Diffraction patterns indicate the stages of transformation [Etoh & Shimada, 1993].

Amorphization rate increases as temperature decreases, as neutron flux increases, and as SPP size decreases. Literature evaluation therefore needs to be compared to reactor and material conditions of specific interest.

The fluence required to produce complete amorphization depends on damage rate (neutron flux), temperature and SPP size, but for typical $Zr(Fe,Cr)_2$ SPPs of initial size near 0.1 µm, the entire SPP is amorphous by end of bundle life burn ups, <50 MWd/KgU (1×10^{22} n/cm^2, E>1 MeV). Interestingly, under well controlled conditions of flux and temperature, the amorphization rate of $Zr(Fe,Cr)_2$ in Zircaloys can be used to estimate the neutron fluence using an equation F = RT where F is the fluence, T is the amorphous rim thickness and R is the experimentally determined amorphization rate. For irradiation temperature near 300°C (573K) in a BWR, the value of R is very approximately 10^{20} (n/cm^2, E > 1MeV)/nm. [Motta & Lemaignan, 1992] and [Bajaj et al, 2002].

For the Zr-Nb type alloys neither the βNb or $Zr(Nb,Fe)_2$ SPPs become amorphous for irradiation temperature >330°C (603K). However, at 60°C (333K) $Zr(Nb,Fe)_2$ does become amorphous at high fluencies.

The process is portrayed schematically in Figure 1-26.

For both Zircaloy-2 and -4 the $Zr(Fe,Cr)_2$ Laves SPPs amorphize and dissolve continuously with fluence. Fe from the amorphous region enters the matrix and diffuses away rapidly while the Cr remains in place. For fluence as low as $2\text{-}4\times10^{21}$ n/cm^2 (E>1MeV), most of the Fe has left the outer rim. This is illustrated in Figure 1-27 and Figure 1-28 for Zircaloy-2 [Takagawa et al, 2004].

1.5 Dislocation loops

In reactor structural materials like Zircaloy, the overwhelming majority of defects are caused by neutrons, and the most important type of defect is the dislocation loop. Two types of loops predominate: <a> and <c> loops. The <a> loop lies on a prism plane and has a Burgers vector in the a-direction of the HCP lattice. Some important characteristics are listed below. Both vacancy and interstitial loops exist. They are very small (10-nm "black spots"), and, even in the transmission electron microscope (TEM), are difficult to analyse.

<a> loops characteristics

Nature	Vacancy (excess), interstitial
Size	8 – 20 nm (80 - 200 Å)
Density	8×10^{14} m^{-2}
Saturation Fluence	1×10^{21} n/cm^2 (E > 1 MeV)
Thermal Stability	To ~400°C (673K)
Effects	Strength, ductility, growth, H solubility (?)

<a> loops form early in the irradiation and the number density reaches a saturation value at a fuel burn up less than 5 GWd/MT. The size of the loops increases with irradiation temperature, and the loops become unstable (start to disappear) at about 673K (400°C). They have a strong effect on mechanical properties, as discussed in Section 1.7 and Section 1.8.

The <c> type of loop lies on the basal plane and has its Burgers vector, or at least a strong component of it, in the c-direction of the HCP cell. As indicated below, unlike the <a> loop, it is strictly a vacancy-type loop, is relatively large (>100 nm), and does not form until considerable irradiation effects have occurred. In Zircaloy, <c> loops are first observed by TEM at a burn up of around 3×10^{21} n/cm^2 (15 GWd/MT) and increase in number density the rest of the fuel lifetime. They are thermally stable to high temperature > 560°C (833K). <c> loops are thought to strongly influence irradiation growth behaviour, and probably do not affect mechanical properties. Their influence on irradiation creep is uncertain. In order to "see" these loops in the TEM, they must be viewed on edge; thus they appear as straight lines in the TEM image. Such <c> loops do form readily in all zirconium alloys, but in fewer numbers in those having additions of Nb or Nb and Fe.

<c> loops characteristics

Nature	Vacancy
Size	> 100 nm (1000 Å)
Density	0.5×10^{14} m^{-2} (mid-range fluence)
Incubation Fluence	3×10^{21} n/cm^2 (E > 1 MeV)
Thermal Stability	Stable to > 560°C (833K) Form at > 200°C (475K)
Effects	Growth, creep, H solubility (?)

As indicated, the kinetics of formation of <a> and <c> type loops differ. The density of <a> type dislocations builds up quickly and saturates at a fluence less than 1×10^{21} n/cm^2 (E > 1 MeV). It appears that a fluence-incubation period exists before <c> type loops begin to form at about 3×10^{21} n/cm^2 (E > 1 MeV) for typical reactor temperatures.

For a straightforward review of the relation between irradiation-induced microstructure and Zircaloy properties, see [Adamson, 2000], where more technical details and references can be found. Reviews are also in ZIRAT reports. e.g., ZIRAT10 STR "Impact of Irradiation on Material Performance" [Adamson & Cox, 2005].

1.5.1 <a> component dislocation loops

The early Ni bombardment studies of [Lee & Koch, 1974] and [Adamson et al, 1974] at high dose rates (>10^{-2} – 10^{-4} dpa/s) and temperatures between 300-500°C (573-773 K) did identify damage with <a> loop type contrast, especially below 400°C (673 K). However the damage characterisation was not clearly defined. [Yang et al, 1987] used very high temperature (470°C (743 K)) and N-ions at a reported dose rate of 5×10^{-3} dpa/s. Doses were 6-77 dpa, but no loops were observed.

[Hellio et al, 1988] conducted experiments in a HVEM using 1 MeV electrons. Temperatures were very high 400-700°C (675-973 K) and dose was very low, <0.2 dpa. Loops lying on prism planes and having <a> type Burgers vectors were observed in pure and impure Zr and alloys. Interestingly, the large loops which could be analysed were all interstitial-type. Loop density was a strong function of temperature (Figure 1-34).

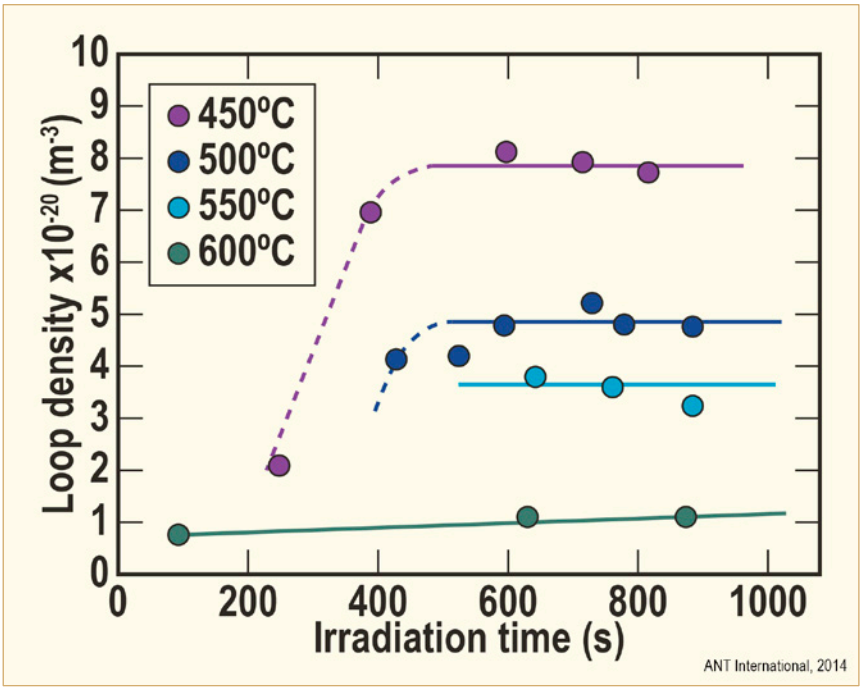

Figure 1-34: Influence of electron irradiation temperature on loop density in pure Zr (400 ppm Oxygen), after [Hellio et al, 1988].

Of more interest, perhaps, it was shown that oxygen (O) had a strong influence on loop growth (Figure 1-35). Addition of Nb also had a small influence on loop growth. The conclusion was that alloying elements and impurities, particularly oxygen, alter the dislocation loop behaviour: nucleation, growth and recovery.

1.6 Irradiation creep and growth

In-reactor experiments to determine creep and growth behaviour are lengthy and expensive. Also experimental variables are difficult to control. Therefore a few experiments have used proton bombardment to sort out some details.

Experiments by [Chapman et al, 1984] and [Chow et al, 2004] used high-energy protons (3.5 and 4.4 MeV) and specimen thickness of 50 µm (0.05 mm) to allow protons to pass through the specimen and create fairly uniform damage within the specimen. The proton beam is rastered across the specimen gauge area, 25 mm × 4 mm.

[Chapman et al, 1984] calculated ion accelerator damage rates using codes available at the time. Figure 1-63 gives an example of depth of penetration into Zr for 3.5 MeV protons. For a 50 µm thick specimen, hydrogen (protons) would not accumulate in the specimen. [Chow et al, 2004] used [Chapman et al, 1984] results for their 4.4 MeV protons, which would be conservative concerning specimen thickness. Damage is varied by controlling the proton beam current.

Table 1-9 gives details of the two tests being discussed.

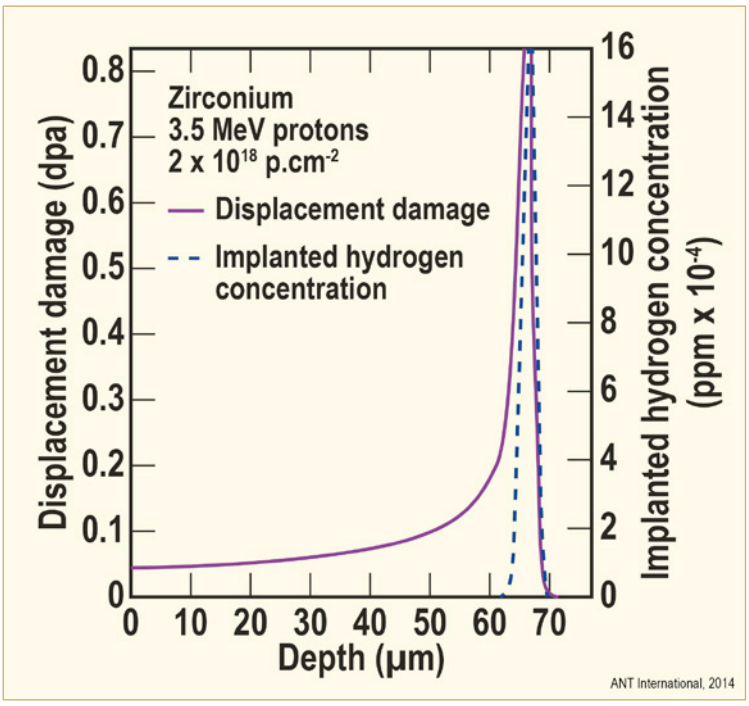

Figure 1-63: Variation of displacement damage and implanted hydrogen concentration (range) with depth for proton irradiated zirconium, after [Chapman et al, 1984]

Table 1-9: Testing Details

Author	Material	Grain size µm	Stress MPa	Damage rate dpa/s ×10^7	Temperature °C	Max dose dpa
[Chapman et al, 1984]	RXA Zircaloy-2	45	0-267	0.5-7	240-340	1.44
[Chow et al, 2004]	CWSR Zirconium	2	50	1.4-6.9	74	0.57

ANT International, 2014

[Chow et al, 2004] conducted low temperature tests (347K, 74°C) on Zr having original low (5 ppm) and moderate (70 ppm) iron (Fe) concentrations. No differences in creep performance occurred due to Fe. It was noted during testing that when the beam current was reduced temporarily to zero, the creep rate was reduced to zero. Typical creep curves are given in Figure 1-64. The dose rate (ϕ) was changed several times during the test; therefore the smooth curve indicated the strain rate is only a weak function of dose rate. If

Eq. 1-3: $$\varepsilon = K\phi^M$$

where ε = creep rate

K = constant

ϕ = dose rate

Then M = 1.1 from the data analysis.

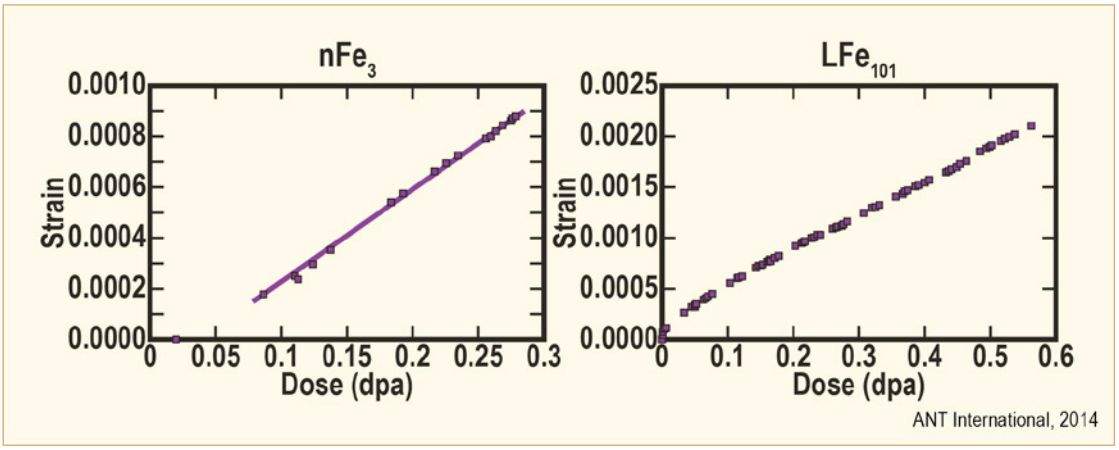

Figure 1-64: Strain as a function of dose for specimens of different Fe content. (nFe_3= 70 ppm; LFe_{101}= 3 ppm), after [Chow et al, 2004].

[Chapman et al, 1984] conducted both irradiation growth (by definition, stress = 0) and creep tests, and made the common assumption that they were independent phenomena. Growth measurements were made in the longitudinal (rolling) direction (f_L = 0.13) of the RX Zircaloy-2 plate with an unavoidably applied stress of 2 MPa[6]. Figure 1-65 compares p-irradiation growth data (damage rate about 4×10^{-7} dpa/s) with in-reactor data (damage rate about 9×10^{-8} dpa/s) from [Williams et al, 1984]. It is noted:

- The total dose is very low, $<2\times10^{-1}$ dpa, equivalent to about 1×10^{20} n/cm^2 (E>1MeV) in a PWR. This is in a very early stage of growth, as evidenced from Figure 1-66 for the bulk form of the same material as used by [Chapman et al, 1984].
- The growth magnitudes and rates between p-irradiation and in-reactor neutrons appear to be similar.
- The effect of dose (displacement) rate appears to be small.

[6] Recent experiments by [Hengstler-Eger et al, 2012] (see Section 1.5.2) indicate that an applied stress can influence formation of <c>loops during ion irradiation; however, <c>loops are not expected to form at the low doses of the [Chapman et al, 1984] experiments.

1.7 Hardness

Hardness measurements have been conducted to evaluate the effect of ion bombardment on mechanical properties. Neutron irradiation is known to induce hardening in zirconium alloys beginning at very low fluence (<1 dpa), increasing rapidly with fluence but achieving a pseudo-saturation by about 2 dpa, as illustrated in Figure 1-79. There is a correlation in hardness to build up of radiation damage in the form of "black spots" and <a> component dislocation loops, which also saturate near 2 dpa. [Griffiths et al, 2007] have shown that hardening actually begins before the fluence/dose at which dislocation loops form, as determined by X-ray line broadening (Figure 1-80). Ultimate tensile strength (UTS) and failure strain also saturate with neutron fluence as shown in Figure 1-81 [Wei et al, 2008]. Hardness measurements are surface-sensitive, so care must be taken that the surface layer being measured is representative of the bulk material of interest. Micro-hardness is usually measured by one of two techniques – Brinell and Vickers hardness. Their results are approximately equivalent. Also hardness can be quantitatively related to trends of UTS. For details of hardness measurement techniques see Section 4 in [Adamson et al, 2013].

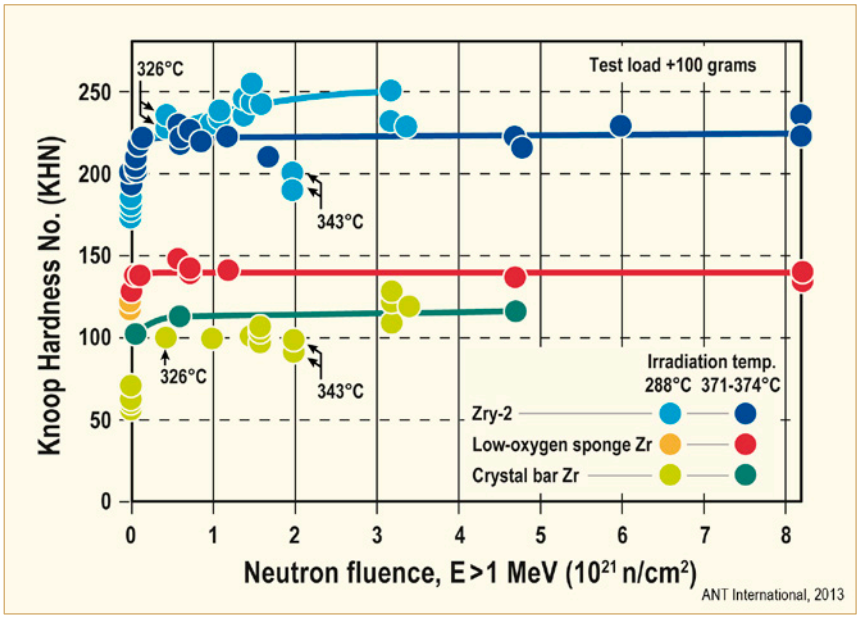

Figure 1-79: Knoop micro-hardness vs. fast neutron fluence for zirconium and Zircaloy-2, after [Tucker & Adamson, 1984].

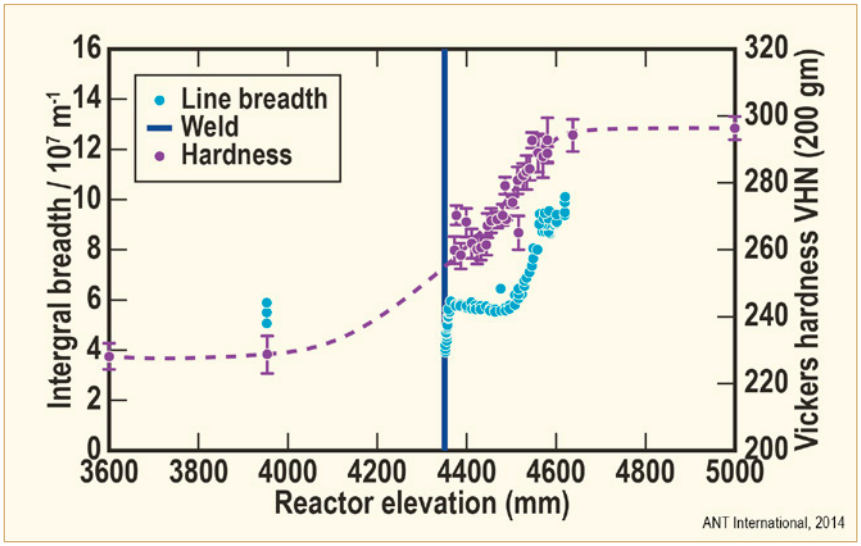

Figure 1-80: Vickers Hardness increase before clear indication of dislocation loop formation (as shown by X-ray line broadening), after [Griffiths et al, 2007].

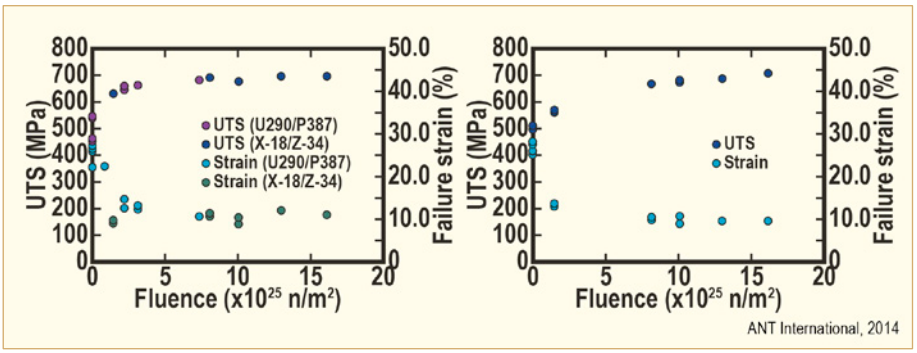

Figure 1-81: Tensile (UTS) strength and failure strain of RXA Zircaloy-2 as a function of fluence at 25ºC (298K), left, longitudinal orientation and right, transverse orientation, after [Wei et al, 2008].

For most ion bombardment experiments the depth of penetration is too small to allow a reliable hardness measurement (see Section 1.2.2) for damage depth of various ions). However, proton irradiation produces a fairly uniform damage over a depth from 0-50 µm, depending on proton energy. [Zu et al, 2005] and [Fournier et al, 2009] used 2 MeV protons in Zircaloy-2 to produce uniform damage over about 20 µm. Using a 10 g load for a Vickers micro-hardness device [Zu et al, 2005] determined the depth of the micro-hardness indentation to be around 1.25 µm, which is small enough to get a good readings in the damage layer. [Fournier et al, 2009] in a very similar experiment used a load of 25 g, which reduces data scatter, and likely produced reliable measurements.

Figure 1-82 gives the [Zu et al, 2005] data, compared to some neutron irradiation data from [Shimada & Nagai, 1983]. [Fournier et al, 2009]'s data point at 2 dpa bombardment temperature of 305°C (578 K) is also indicated.

Table 1-11: Effect of proton irradiation at 350°C (623 K) on loop density and size, after [Zu et al, 2005].

	As received	2 dpa	5 dpa	7 dpa
Average diameter, (nm)	0	7	11	11
Density (10^{21} m^{-3})	0	7	8	15
				ANT International, 2014

1.8 Deformation

It is known that neutron irradiation affects deformation modes in zirconium alloys, changing relatively uniform deformation on prism planes to highly localized deformation on prism or basal planes. This phenomenon, called dislocation channelling, was reviewed in Section 4 of the ZIRAT15 Annual Report [Adamson et al, 2010]. One of the consequences of dislocation channelling is reduced macroscopic strain to failure and formation of intense shear bands during tensile testing of standard specimens. It also has been shown [Lee & Adamson, 1977] that iodine stress corrosion crack (ISCC) initiation is enhanced in the shear bands, where avalanches of dislocations within the channels emerge from the surface.

[Fournier et al, 2009] used 2 MeV proton irradiation at 305°C (578 K) to assess the effect of surface irradiation damage on channelling and ISCC. Mini-tensile specimens were 1.5 mm thick and had a uniform proton damage layer about 25 µm deep (see proton range in Section 1.5.2) to about 2 dpa. TEM exams showed dislocation channelling behaviour (Figure 1-83) very similar to that observed in neutron irradiated Zircaloy; that is, predominantly basal channelling as reported by [Onimus et al, 2004] and the CEA group, and only minor prism channelling that was reported by [Adamson & Bell, 1985] and the GE group.

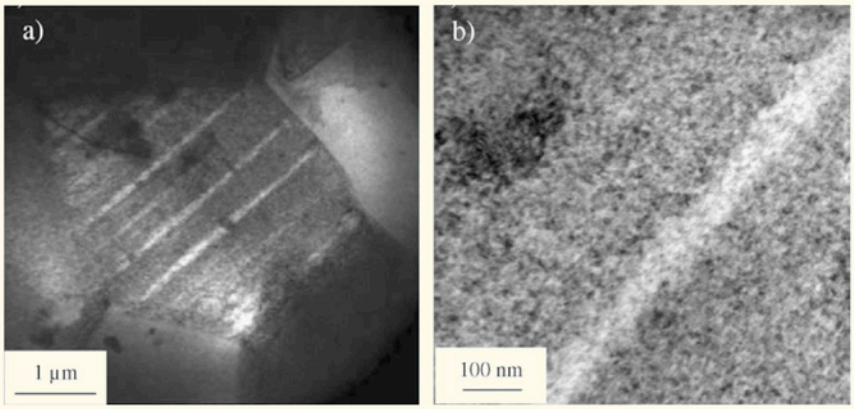

Figure 1-83: TEM micrographs of dislocation channels in Zircaloy-4 proton irradiated at 305°C to 2 dpa and strained to 0.5% macroscopic plastic strain at room temperature [Fournier et al, 2009].

Proton irradiation was found to strongly promote ISCC, but no direct correlation could be made between basal channelling and ISCC. Despite impressive use of finite element analysis (FEA), it is clear that stress-strain analysis of the complicated system is difficult at best. But overall, proton bombardment proved to provide a good simulation of neutron irradiation.

1.9 Solutes and phases

[Woo et al, 2000] and [Woo et al, 1995] used 10 MeV electrons to study phase reactions in Zr2.5Nb. (The driving force was CANDU corrosion, see Section 1.10). The high energy electrons have high range (up to 8 mm) in zirconium so surface effects are minimized compared to 1 MeV electrons in a HVEM. Electrons were produced by pulsed electron linac (PHELA) at AECL, Chalk River. On average the damage rate is low (1.3 dpa in 370 h, or 1×10^{-6} dpa/s) but the instantaneous damage rate is high, about 10^{-3} dpa/s. Temperature was between 410-450°C (683-723 K).

[Cann et al, 1993] used 3.6 MeV protons to study precipitation in Zr2.5Nb. The proton range was higher than the foil thickness (50 µm) to minimize "contamination" with hydrogen. The damage rate was estimated to be about 5×10^{-7} dpa/s. Temperature was 447°C (720 K) and dose was about 1 dpa.

[Motta et al, 1996] used 350 KeV Ar ions and 900 KeV electrons to study precipitation in Zr with 12 or 20% Nb added. Temperatures were 300-400°C (573-673 K) and doses were up to 5 dpa. TEM and bombardments were done simultaneously (in-situ).

The electron and proton irradiations resulted in formation of needle-like βNb precipitates in the alpha phase of the Zr2.5Nb specimens. An example, for 440°C, is given in Figure 1-84. At the lowest temperature, 410°C (683 K); small <a> loops having vacancy character were also formed. The lower temperature Ar bombardments produced no new identifiable phases.

Neutron-irradiated Zr2.5Nb was shown to form similar βNb precipitates [Coleman et al, 1980]. Irradiations were at 297-497°C (570-770 K) to about 0.7 dpa. It appears that proton and electron irradiations can provide at least some information useful for understanding the effects of reactor irradiation on the microchemistry (and corrosion) of Zr2.5Nb.

It is noted that formation of needle-like βNb precipitates during reactor irradiation of Zr1Nb alloys has often been observed, a recent example being [Doriot et al, 2013].

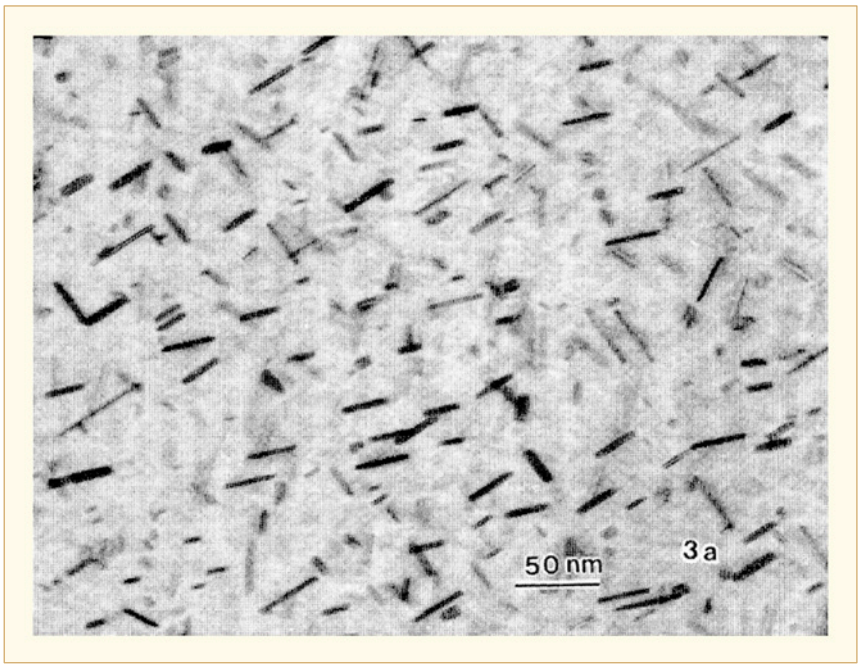

Figure 1-84: The microstructure of Zr2.5Nb electron-irradiated at 440°C (713 K) to 1.3 dpa showing needle-like precipitates in the alpha-Zr interior. [Woo et al, 2000]

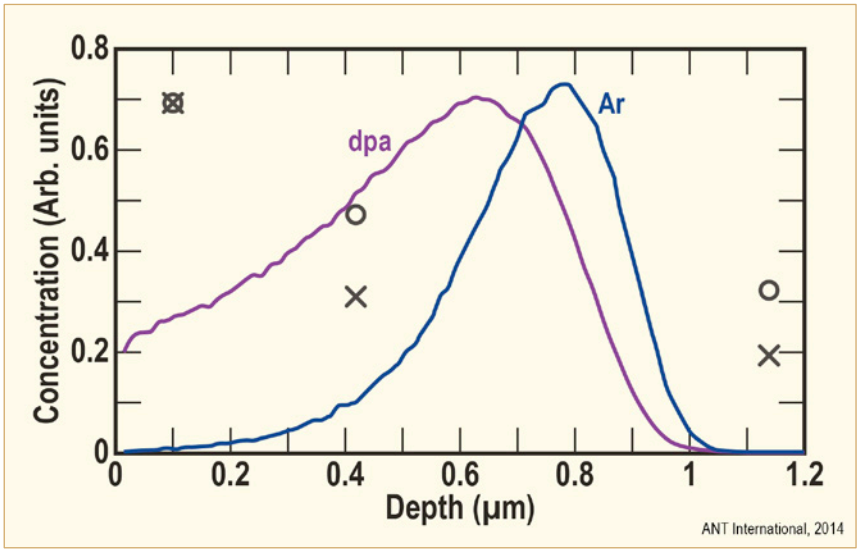

Figure 1-86: The depth distributions (TRIM) of dpa and Ar in Zr after 1.5 MeV AR^{+1} irradiations. Open circles and crosses give relative differential concentrations of Fe and Ni in Zry-2 420ºC (693 K) irradiation. Dose is 10-30 dpa, after [Zou et al, 1995].

1.10 Corrosion

1.10.1 Zircaloy - proton bombardment

Corrosion resistance of Zircaloy-2 and -4 is significantly affected by neutron irradiation. Of particular importance is the effect of irradiation on the second phase precipitates (SPPs) and on the balance between Fe, Cr and Ni in the SPPs and in the zirconium matrix. Such effects are covered in several ZIRAT reports, including [Adamson & Cox, 2005] and [Adamson et al, 2007] and the current ANTI Academy on Corrosion, 2015. Examples of results are given in [Cheng et al, 1994], where it is shown that neutron irradiation, due to its effect of increasing the amount of Fe, Cr and Ni in the matrix by SPP dissolution, dramatically increases uniform corrosion and decreases nodular corrosion. Also, [Etoh et al, 1991] demonstrated elimination of nodular corrosion by neutron irradiation, and its return after post-irradiation thermal annealing. It is postulated, based on experiments, that elimination of nodular corrosion can be caused by only a small increase in the solute concentration in the matrix, on the order of 200 ppm [Cheng & Adamson, 1987], [Kruger et al, 1992] and [Kai et al, 1992] demonstrated similar effects using 1 MeV proton irradiation at 350ºC (623 K). Sub-surface damage was low (0, 0.01, 0.1 and 1.0 dpa). TEM exams were conducted at 2 µm depth following the dose plot of Figure 1-87. Post-bombardment corrosion tests were conducted in steam at 500ºC (773 K), 1500 psi, which is a nodular corrosion test similar to those mentioned above for neutron-irradiated material. Even the lowest dose eliminated nodular corrosion, as shown in the optical micrographs of Figure 1-88 and the weight gain plots of Figure 1-89.

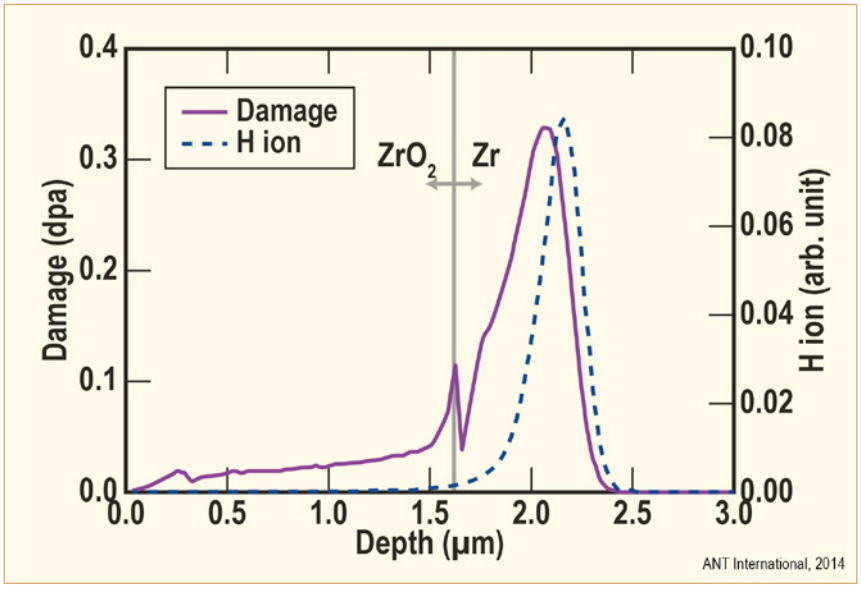

Figure 1-93: SRIM calculation of lattice displacement and hydrogen concentration in ZrO_2 and Zr by 350 KeV proton (H^+) ion bombardment, after [Une et al, 2012].

1.11 Surface embrittlement

During typical light water reactor (LWR) service, the inner surface of the Zircaloy cladding tubes receives a high dose of high energy fission products. As reported by [Schuster & Lemaignan, 1988] this results in a damaged surface layer about 10 µm deep with more than 2% foreign atoms at standard burn up. [Schuster & Lemaignan, 1988] simulated the fission product effect by bombarding at about 330°C (603 K) with 98 MeV Kr ions having a range of about 10 µm zirconium. Dose was several dpa. Tensile tests were conducted on both Zircaloy and zirconium to determine the effect on surface embrittlement. Indeed, surface embrittlement was observed in the form of a high density of cracks in the bombarded surface after only minor imposed plastic deformation. The effect was less significant for Zr than for Zircaloy.

Such tests appear to be useful for determining crack initiation sites for SCC during pellet-cladding-interaction (PCI) events, and for explaining the beneficial effects of Zr liners in BWR fuel.

Irradiation hardening in pure hydrides was investigated by [Oono et al, 2013]. Hydrides in δ-Zr or ε-Zr phases were bombarded with 6.4 MeV Fe. Figure 1-94 shows the Fe ions concentrate at a depth of about 2 µm, which corresponds to the SRIM calculations.(See paper for full details) Micro-hardness measurements of the bombarded surface used a small load of 30 mN (3 grams), but penetration of the indenter is not described in the paper. Hardness results are shown in Figure 1-95, in which it is seen that δ-hydride is harder than ε-hydride. Ion bombardment did not change the deformation modes in either phases. Slip and twinning were observed, but defects, Figure 1-96, introduced by the Ni ions increased the resistance to deformation. This paper gives excellent new information on hydrides.

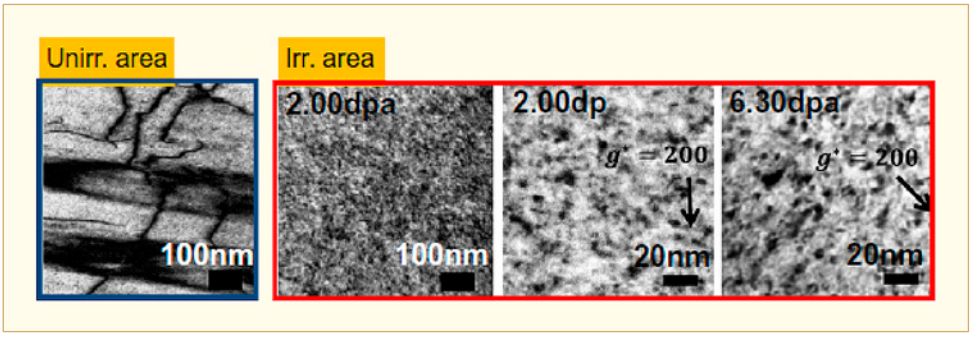

Figure 1-96: TEM images showing irradiation-induced defects in δ-Zr hydrides bombarded with Ni ions [Oono et al, 2013].

Another paper [Janse van Vuuren et al, 2013] examines the effect of ion bombardment of nano-crystals having potential use in fast reactor fuel. Although beyond the scope of the current review, the interested reader may find the experimental procedures and results interesting and/or useful.

1.12 Facilities

Table 1-13 lists Facilities currently available for ion bombardment studies. Caution: this list may not be up-to-date or complete.

Table 1-13: Current ion bombardment facilities.

Paper	Country	Location	Facility	Comment
[Tournadre et al, 2011, 2013a], [Zu et al, 2005], [Fournier et al, 2009], [Hengstler-Eger et al, 2012]	USA	University of Michigan	Michigan Ion Beam Laboratory	Protons
[Idrees et al, 2013b], [Hengstler-Eger et al, 2012, 2014], [Zu et al, 2005]	USA	Argonne National Laboratory	ANL IVEM-Tandem Facility	Ions
-	England	Manchester University	Dalton Nuclear Institute, Dalton Cumbria Facility	Ion Protons
-	Canada	Queen's University	Reactor Materials Testing Laboratory	Protons
[Sarkar et al, 2008]	India	Kolkata	Variable energy Cyclotron	Ions
[Oono et al, 2013], [Janse van Vuuren et al, 2013], [Une et al, 2012]	Japan	Kyoto University	Van de Graff (4 MeV)	Ions, electrons
[Hengstler-Eger et al, 2012, 2014]	Germany	Technische Universität, München	IPP, MLL tandem accelerator	Ions
[Tournadre et al, 2011, 2013a], [Pêcheur et al, 1994], [Hellio et al, 1988]	France	CSNSM/IN2P-Orsay	IRMA, ARAMIS	Ions
[Yamada & Kameyama, 2012]	Japan	JAEA-Takasaki	TIARA	Protons, ions
-	US	U. of Wisconsin, Madison	Ion beam laboratory	Protons, ions
				ANT International, 2014

1.13 Summary and conclusions

In reactor experiments (neutron irradiation) provide information very relevant to component operation. However, such experiments are time consuming, expensive, and create highly radioactive material (specimens). Ion bombardment (IB, ion irradiation, charged particle irradiation) simulations can shorten the time, lower the cost and minimize radioactivity. However, IB produces only tiny amounts of material to test or examine, and legitimate questions arise about the applicability of such data to actual reactor performance.

Starting in the early 1970s, IB was used to study void formation in fast reactor materials and since then has been used sporadically to explore irradiation effects on various materials.

For Zr-alloys a few IB experiments were conducted between 1966 and1974, interest increased in the 1980s peaked in the 1990s and then dropped off in the early 2000s. Since 2010, over 14 IB experiments were published with the apparent interest continuing to increase to date. New experimental facilities are being constructed in at least England and Canada, and use at existing facilities at University of Michigan, Argonne National Laboratory and others are apparently expanding.

<u>Application on ion bombardment techniques is expanding.</u>